AMQ

STABLE ISOTOPE STRATIGRAPHY OF TRAVERTINE SEQUENCES
FROM CHANNEL DEPOSITS AT HIERAPOLIS OF PHRYGIA (DENIZLI, TURKEY)

Asmaa Fayek [1], Mauro Brilli [2], Nicolas Guyennon [3], Francesca Giustini [2], Mario Voltaggio [2]

1 Geology Department, Faculty of Science, Helwan University, Cairo, Egypt
2 IGAG, CNR, Roma, Italy
3 IRSA, CNR, Roma, Italy
Corresponding author: M. Brilli <mauro.brilli@cnr.it>

ABSTRACT: Travertine sequences from petrified channels used in antiquity as water supply canals in the city of Hierapolis (Denizli, Turkey) for irrigation and domestic use were sampled and analyzed for stable isotopes composition. Data records from two channels show composite quasi-periodic variations. Radium-226 activity was measured to calculate temporal constrains; one of the channels, 182cm thick, deposited in 790±71 years, whereas the other, 644cm thick, in 995±71 years. Isotope data, studied through spectral and cross-spectral analysis, indicate that the different oscillation frequencies may be related to surface temperature and rainfall pulses.

KEYWORDS: Isotope stratigraphy, petrified channels, Hierapolis of Phrygia

1. INTRODUCTION

Aerial views and satellite images are definitely the best point to understand how the urban and suburban landscape of Hierapolis of Phrygia is strongly characterized by the presence of travertine channels (Scardozzi, 2013); the dense network that they draw in some areas of the city and outside had already been perceived as an element connoting the topography of the place by the scholars who visited the remains of the city in the nineteenth century and represented it schematically in maps and some views (e.g., Trémaux, 1958).

The travertine channels of Hierapolis originate from thermal springs on the terrace on which the city was founded. They consist of continuous calcareous deposit which has grown over the centuries, often reaching impressive forms today (Hancock et al., 2000; Özkul et al., 2002).

The complex network of travertine channels is divided into two distinct groups from the topographic and chronological point of view (Di Taranto, 2015). The remains of those canals that descend from the city's terrace towards the fields of the underlying Lykos valley can be referred to the oldest group; these channels had the dual function of irrigation and delimitation of agricultural land. They are still preserved today for long distances and with remarkable heights (up to 10 m). The exact location of the springs that fed these canals is not known, but it is possible that they could be found along the edge of the terrace.

The most recent group, datable to the Middle-Byzantine period, is constituted of a network of travertine channels developed within the urban area. The archaeological excavations have confirmed its use between the mid-seventh century AD and about the 1354 AD when an earthquake caused the definitive abandonment of the city. From the urban area the waters flowed towards the valley, partly exploiting the oldest conduits, thus contributing to increase the carbonate accretion, which generated, in the course of the following centuries, the monumental canals we see today.

Travertine channels are highly interesting constructions, since they are related to human activity. These deposits are often linked to thermal springs. Their formation is a consequence of the thermal shock induced by the differences between water and air temperatures that accelerate dissolved carbonate precipitation, producing huge bodies. The kinetics of this cooling are a function firstly of thermal water/air contrast, and secondly of the distance from the spring. Jimenez et al. (2006) isotopically studied this peculiar travertine deposits at Alicùn de las Torres (Granada, Spain) where active channels are still growing.

In the present study, two channels were selected for isotope stratigraphy. Their rapid accretion allows evaluation of climatic variations at decadal scale resolution.

2. MATERIALS AND METHODS

Two travertine channels (B and C) were sampled continuously along the central axis of their vertical section where cut surfaces are exposed (fig. 1); before the sampling, a carbonate layer, a few centimeters thick, was scraped to eliminate the external surface exposed to the atmosphere. Channel B is located inside the urban area at about 300m away from the closest spring orifice, with a height of 183cm. On contrast, travertine channel C is situated on the steep slopes in the north west side of Hierapolis. This channel has grown as high as around 10m; it was sampled for 644cm from the top.

Oxygen and carbon isotopes measurements were performed on a total of 655 samples from channel B and 182 samples from channel C by using acid digestion technique (Gasbench II (Thermo) on line with a Delta Plus mass spectrometer). Results were expressed in delta per mill versus V-PDB standard.
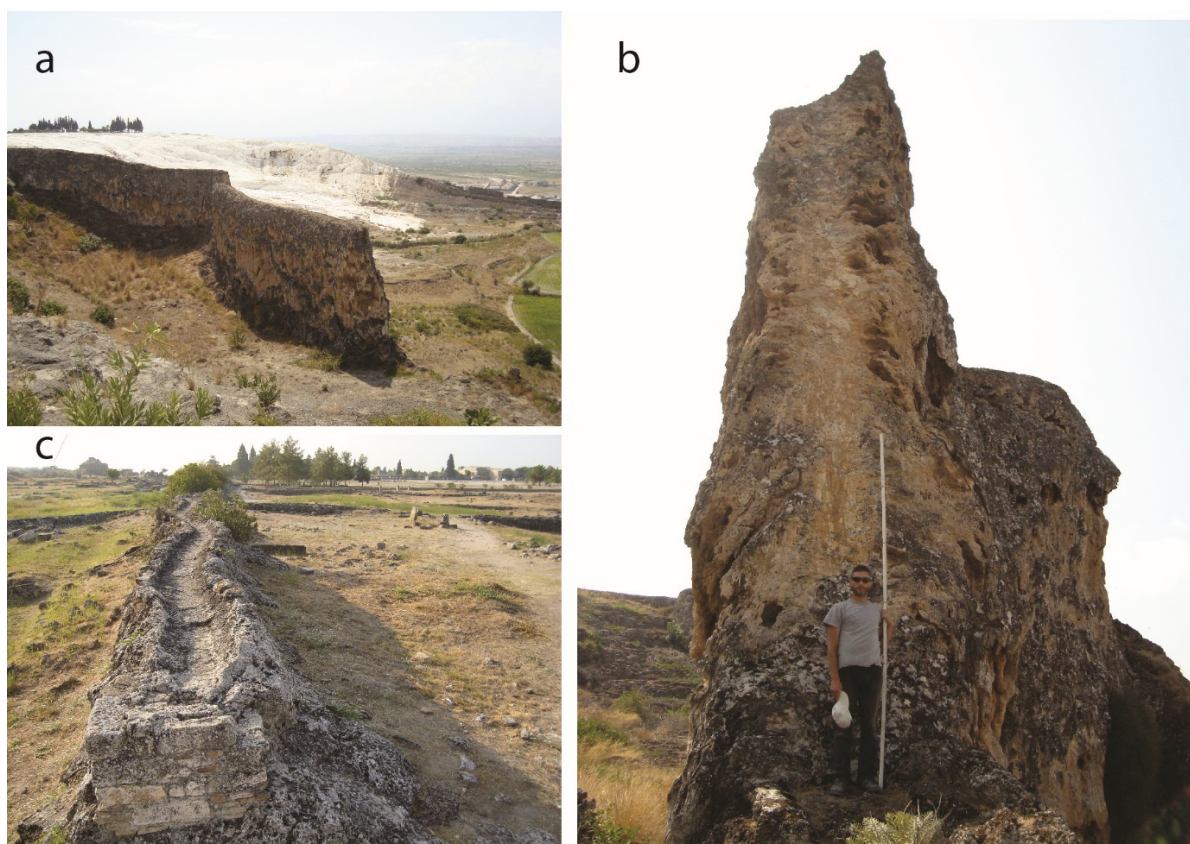
Fig. 1 - Petrified channels at Hierapolis. a) Panoramic view; b) cut surface along Channel C (the bar is 3 m long); c) Channel B is the main collector which runs NW – SE through the ancient city of Hierapolis.

The sequences were temporally constrained by the dating method based on the decay of Radium-226; the details of this method are described by Romano et al. (1987).

3. RESULTS AND DISCUSSION

Dating

Archaeological information provided some constraints to the time of deposition of the travertine channel bodies. The upper temporal limit of the activity of the channels can be placed around 1354 AD, when a strong earthquake caused the destruction of Hierapolis. Channel B rests on a pavement of the VII century, whereas the bottom of channel C surely dates back to the Roman imperial times (Di Taranto, 2015).

^{226}Ra dating method allows the definition of a time interval between two points selected within the sequence. Analyses for ^{226}Ra ^{230}Th, ^{232}Th and ^{238}U activities were run on two samples from channel B (at the top and bottom of the sequence), and on three samples from channel C (at the top, bottom and 380cm from the bottom).

Formulation of the equations for ^{226}Ra method is based on the widely used U-Th methods with the further introduction of ^{230}Th to ^{226}Ra decay. Two sources contribute to the activity of ^{226}Ra: (i) ^{226}Ra originally deposited in the calcite, and (ii) ^{226}Ra in equilibrium with ^{230}Th,

leached from silicatic residue during acid attack (non-carbonatic ^{226}Ra). The difference between the total ^{226}Ra activity, measured in our samples, and non-carbonatic ^{226}Ra activity gives the ^{226}Ra excess. The initial activity of ^{226}Ra is not known, but assuming it remained constant during the deposition of the travertine sequence it is possible to have the age difference at different levels. The following equation was used to estimate the age difference from ^{226}Ra$_{excess}$ ratio between two samples collected at different levels of the sequences:

$$226Ra_{excess}(t) = 226Ra_{excess}(o) \times e^{-\lambda 226t}$$

where ^{226}Ra$_{excess}$ (t) is the excess of Radium at time t, ^{226}Ra$_{excess}$ (o) is the initial activity of ^{226}Ra, λ is the ^{226}Ra decay constant. The difference between this equation at time t1 and the same equation a time t2, which represent two levels of the sequence, gives the equation of age difference (Δt):

$$\Delta t = \frac{ln\frac{226Ra_{excess}(t1)}{226Ra_{excess}(t2)}}{-\lambda 226}$$

^{226}Ra$_{excess}$ is calculated from the difference ^{226}Ra - ^{230}Th, assuming secular equilibrium between ^{230}Th and ^{226}Ra

	^{230}Th (Bq/kg)	^{226}Ra (Bq/kg)	^{226}Ra$_{ex}$ (Bq/kg)	^{232}Th (Bq/kg)	^{238}U (Bq/kg)
Ch_B (top)	0.72±0.02	4.57±0.07	3.85±0.07	0.81±0.02	6.0±0.03
Ch_B (bottom)	3.58±0.05	6.32±0.06	2.74±0.08	4.12±0.06	6.0±0.03
top/bottom ratio					0.71±0.02
Δt					*790±65*
Ch_C (top)	0.45±0.01	4.31±0.07	3.86±0.07	0.71±0.02	3.8±0.2
Ch_C (middle)	0.18±0.01	3.41±0.07	3.23±0.07	0.13±0.01	3.9±0.2
Ch_C (bottom)	0.41±0.01	2.93±0.07	2.52±0.07	0.63±0.02	3.8±0.2
top/bottom ratio					0.65±0.02
Δt					*995±71*
middle/bottom ratio					0.84±0.01
Δt					*571±71*

Tab. 1 - Age difference (Δt) in years between the levels where samples of channel B and C were selected. Sample collected from the middle of channel C was at 3.80 m from the bottom. ^{230}Th, ^{232}Th were determined by isotope dilution alpha spectrometry, ^{226}Ra and ^{238}U were determined by high resolution gamma spectrometry.

in the non-carbonatic component.

In table 1 are listed the results of the spectrometric analysis and the Δt calculated in channels B and C.

Stable isotopes

Isotope records were converted from data versus thickness to data versus time using the results given by the Radium-226 chronology (Fig. 2 and b). The relative time vector (T*) associated to the δ^{18}O and δ^{13}C series has been obtained using a linear piecewise interpolation of available durations, under the hypothesis of constant rate of deposition, and setting to 0 the top of the sequences.

On initial consideration, the records B and C show low amplitude, composite cyclic variations for both carbon and oxygen records. The main issue is to decipher the various, competing factors that drive oxygen and carbon isotope variations, in order to recover unambiguous paleoclimatic signals. δ^{18}O of travertine calcite reflects the temperature and δ^{18}O of the water where calcite deposited. The δ^{18}O of the water may have been varied in the past for different reasons, namely variation in δ^{18}O of meteoric precipitation, mixing between shallow and deep groundwaters, evaporation occurred from the spring orifice to the sampling locations and consequent isotopic disequilibrium during calcite precipitation (Pentecost, 2005; Andrews, 2006; and references therein). δ^{13}C reflects the sources of carbon which contribute to the carbon species in solution, the tendency of CO_2 dissolved in the groundwater to equilibrate with atmosphere and evade at surface emergences, and, subsequently, along the surface flow (Pentecost, 2005; Andrews, 2006; and references therein).

Considering the context of channelized flow of thermal waters and the sampling locations at a certain distance from the springs, the temperature drop is an important factor on which the oxygen isotope composition depends; it also influences the amount of CO_2 evasion (the increase in distance implies a progressive thermal decline). Air temperature induces, when lowers or rises, an increase or decrease in δ^{18}O, whereas δ^{13}C behaves oppositely since higher temperature favors CO_2 evasion leaving behind a residual CO_2 isotopically "heavier" and *vice versa*. This implies that the records of carbon and oxygen isotopes will be negatively correlated when temperature is the main factor to influence isotopes in carbonate formation.

Oxygen isotopes in travertine carbonates may also depend on the variations of oxygen isotope composition of groundwater which is, in turn, derived by meteoric precipitation; isotope ratios in precipitation are averagely lower in cold climates and higher in warm periods, an effect that can be more or less evident in groundwaters according to precipitation intensity. Cold - humid climatic conditions may promote soil biogenic CO_2 formation, resulting in isotopically light carbon isotope ratios. The increased introduction of soil CO_2 into groundwater produces a lowering in the δ^{13}C of the calcite precipitated around the springs. In the case of the area studied this lowering was modulated by heavy carbon CO_2 sources, generated by decarbonation of local bedrock and mantle degassing, of which the local thermal system is rich (Dilsiz, 2006; Kele et al., 2011). These mechanisms, however, generate carbon and oxygen isotope records that co-vary positively.

On the basis of the isotope record profiles, it seems that the factors described above may have influenced recent past waters at Hierapolis thermal springs and the calcium carbonate of the channels. Variations in δ^{13}C seem to correlate positively with δ^{18}O at higher frequency oscillations, whereas negatively at lower frequencies. These evidences may be related to the mechanisms above described: δ^{13}C/δ^{18}O positive covariance can be related to the variation in air temperature, whereas negative covariance to the variations in climate and precipitation regime reflected in groundwater isotopes.

Cross wavelet spectral analysis was applied to study the oscillatory nature of the isotope data records to investigate the different responses in time to climate variations (Fig. 2c).

The mathematical basis of this technique is given by Grossmann & Morlet (1984) and a complete description by Torrence & Compo (1998). The wavelet analysis carried out in this study was performed using the free Matlab-software package (WTC-R16) available at the URL: http://noc.ac.uk/using-science/crosswavelet-wavelet-coherence (Grinsted et al., 2004). A physically consistent definition of energy for the wavelet power spectrum has been adopted following Liu et al. (2007) to
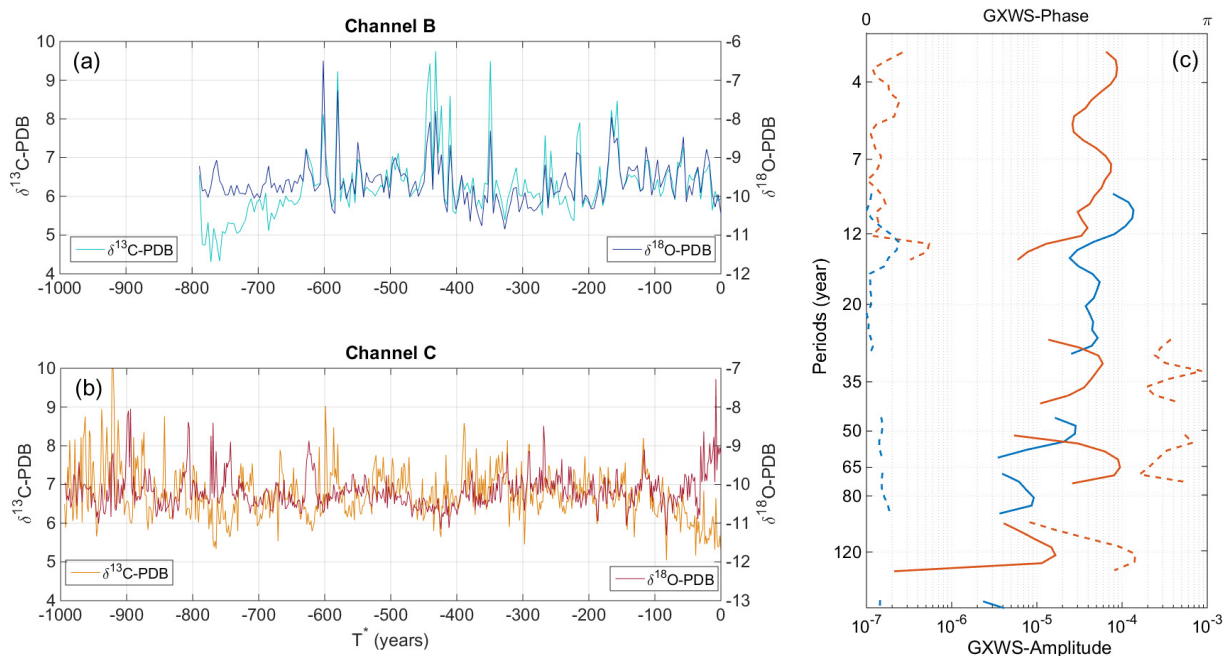
Fig. 2 - Panel (a) presents the δ^{13}C (cyan full line, left axis) and δ^{18}O (blue full line, right axis) time series for Channel B. Panel (b) presents the δ^{13}C (orange full line, left axis) and δ^{18}O (red full line, right axis) time series for Channel C. Panel (c) presents the global cross-wavelet spectrum (GXWS) between δ^{13}C and δ^{18}O in terms of phase (dash line) and amplitude (full line) for Channel B (blue lines) and Channel C (orange lines).

allow a direct comparison of the spectral peaks across scales. Following Guyennon et al. (2014), the associated global cross-wavelet spectrum is defined for amplitude (GXWS-Amplitude) and phase (GXWS-Phase) as the time integration of the significant (p value <0.05) wavelet coefficients. The GXWS Amplitude and Phase gives a synthetic description of the main common signals characterizing the time series.

Wavelet analysis reveals spectral peaks of significant intensity at frequencies corresponding to 7 and 11-12 years, especially evident in sequence C which has higher resolution; for these periodicities the C and O records are prevalently in phase. At lower frequencies in sequence C, it is possible to evidence spectral peaks between 25 – 35 and at 65 years, with C and O records prevalently in phase opposition; whereas in sequence B, peak at 50 years with C and O records in phase.

The periods from 7 to 12 years can represent the response of the data to the aquifer dynamic pulses which, being influenced by meteoric precipitation, are strongly linked to shallow, fast aquifer circulation and to alternation of not only cold/warm climate but also humid/arid conditions. At higher periodicities, around 30 yrs and 65 yrs, the surface temperature oscillation seems to have influenced most the record C. The peak at 50 years recorded in the sequence B should be related to climatic variation filtered by the local aquifer system; this peak is not observed in the record of sequence C. The sampling location of the two channels with respect to the spring orifice are surely different and this may have played a role on this discrepancy; the B sampling site is closer to the spring orifice than the C sampling site, as

indicated from the average carbon isotopic composition of the two channels δ^{13}C = +6.2‰ in B; δ^{13}C = +6.7‰ in C). The carbon isotopic composition of B lower than C may indicate a larger CO_2 degassing effect at site C, therefore a shorter distance traveled by the water to reach the site B. An average 0.5‰ difference, considering the magnitude of amplitude variations observable in the carbon records, can be considered significant to obfuscate the CO_2 evasion effect and recording the CO_2 variations related to the CO_2 mixing occurred in the groundwater system.

4. CONCLUSION

Two sequences reconstructed from travertine channel deposits used at Hierapolis of Phrygia as water collectors were analyzed for carbon and oxygen isotope stratigraphy. The Radium-226 dating method constrained the time interval covered by the sequences revealing that the channel B sequence is shorter in duration (790±71 years) and the channel C sequence is longer (995±71 years). It is likely that the top of both sequences can be dated close to the 1354 AD, when a strong earthquake destroyed the city and led to the abandonment of the area. Isotope records show decadal-scale, pseudo-periodic fluctuations related to climatic variations. The study was facilitated by using cross wavelet spectral analysis to evaluate the most powerful frequencies of oscillation. Air temperature seems to play an important role in influencing the data records; the fluctuations, which seem related to this factor, show periods around 30 and 65 years. Whereas

higher frequency pulses at periodicities of about 7, 10, 12 years seem to be related to the shallow aquifer dynamics. The sequence B shows that climatic oscillations with periods around 50 years can be attributed to the filtering of the aquifer system to air temperature periodic variations.

ACKNOWLEDGMENTS

REFERENCES

Andrews J.E. (2006) - Palaeoclimatic records from stable isotopes in riverine tufas: Synthesis and review. Earth-Science Reviews, 75(1-4), 85-104.

Dilsiz C. (2006) - Conceptual hydrodynamic model of the Pamukkale hydrothermal field, southwestern Turkey, based on hydrochemical and isotopic data. Hydrogeology Journal, 14, 562-572.

Di Taranto I. (2015) - La rete dei canali di travertino. In: Nuovo Atlante di Hierapolis di Frigia VII. Cartogra-Cartografia Archaeologica della Citta e delle Necropoli, Scardozzi G. (ed.), 63-69.

Grinsted A., Moore J., Jevrejeva S. (2004) - Application of the cross wavelet transform and wavelet coherence to geophysical time series, Nonlinear Processes in Geophysics, 11, 561-566.

Grossmann A., Morlet J. (1984) - Decomposition of Hardy Functions to Square Integrable Wavelets of Constant Shape. Journal on Mathematical Analysis, 15, 723-736.

Guyennon N., Valerio G., Salerno F., Pilotti M., Tartari G., Copetti D. (2014) - Internal wave weather heterogeneity in a deep multi-basin subalpine lake resulting from wavelet transform and numerical analysis. Advances in Water Resources, 71, 149-161.

Hancock P.L., Chalmers R.M.L., Altunel, E., Çakir Z., Becher-Hancock A. (2000) - Creation and destruction of travertine monumental stone by earthquake faulting at Hierapolis, Turkey. In: The Archaeology of Geological Catastrophes (McGuire W.G., Griffiths D.R., Hancock P.L., Stewart I.S., Eds.), Geological Society, London, Special Publication, 171, 1-14.

Jimenez de Cisneros C., Caballero E., Jimenez-Lopez C. (2006) - $\delta^{18}O$ and $\delta^{13}C$ of modern/ancient travertines from thermal spring (Alicún de las Torres, Southern Spain). GeoActa, 5, 13-24.

Kele S., Özkul M., Fórizs I, Gökgöz A., Baykara M.O., Alçiçek M.C., Németh T. (2011) - Stable isotope geochemical study of Pamukkale travertines: New evidences of low-temperature non-equilibrium calcite-water fractionation. Sedimentary Geology, 238 (1-2), 191-212.

Liu Y., Liang X.S., Weisberg R.H. (2007) - Rectification of the bias in the wavelet power spectrum. Journal of Atmospheric and Oceanic Technology, 24, 2093-2102.

Özkul M., Varol B., Alçiçek M.C. (2002) - Depositional environments and petrography of Denizli travertines. Mineral Res. Expl. Bul., 125, 13-29.

Pentecost A. (2005) - Travertine. Springer Verlag, Berlin, pp. 446.

Romano R., Taddeucci A., Voltaggio M. (1987) - Uranium-series dating of some travertines from the southwestern flank of Mt. Etna (Sicily). Rendiconti della Società Italiana di Mineralogia e Petrologia, 42, 249-256.

Scardozzi G. (2013) - Nuovi dati sulla topografia antica di Hierapolis di Frigia. Rivista di Studi di Topografia Antica, ATTA 23, 25-59.

Torrence C., Compo G.P. (1998) - A practical guide to Wavelet Analysis. Bulletin of the American Meteorological Society, 79, 61-78.

Trémaux P. (1858) - Exploration archéologique en Asie Mineure, Paris.